2-(2′-Hydroxyphenyl)benzoxazole-Containing Two-Photon-Absorbing Chromophores as Sensors for Zinc and Hydroxide Ions

Yanqing Tian,[†,§] Ching-Yi Chen,[†] Chang-Chung Yang,[†,‡] A. Cody Young,[†] Sei-Hum Jang,[†,§] Wen-Chang Chen,[‡,||] and Alex K.-Y. Jen*[,†,§]

Department of Materials Science and Engineering, Box 352120, University of Washington, Seattle, Washington 98195-2120; Department of Chemical Engineering, National Taiwan University, Taipei, Taiwan 106; Institute of Advanced Materials and Technology, University of Washington, Seattle, Washington 98195; and Institute of Polymer Science and Engineering, National Taiwan University, Taipei, Taiwan 106

Received September 4, 2007. Revised Manuscript Received November 30, 2007

Three new two-photon-absorbing (2PA) chromophores derived from 2-(2′-hydroxyphenyl)benzoxazole (HPBO), having two-photon absorption cross sections up to 530 GM (δ, expressed in GM; 1 GM = 1 $\times$ 10^{-50} cm^4 s $photon^{-1}$ $molecule^{-1}$), were synthesized and investigated as metal ion and pH sensors. These chromophores were designed with an increasing number (0, 1, and 2) of HPBO(s) groups as binding sites for metal ions. Such variations provide a systematic approach to correlate structures with their linear photophysical, sensing, and two-photon absorption properties. The HPBO-containing sensors show unique response for zinc ion. Significant zinc ion stimulated photophysical properties with evident enhancements in fluorescence intensities from both one- and two-photon processes were detected. Moreover, one chromophore having HPBO groups in both terminal ends exhibits significant modulation of fluorescence intensities in response to the phenol group deprotonation in the HPBO moiety. A very large two-photon absorption cross section of 4120 GM, the highest reported for bisphenolate-containing 2PA materials, was measured for the chromophore under basic conditions. The molecular structures have a significant influence on the 2PA properties, which follows a trend of the substitution groups on the HPBO moiety in the order of $-O^-$ > $-OZn$ > $-OCH_2R$. The present study provides a protocol for elucidating the relationship between the photophysical properties and molecular structures.

1. Introduction

The development of novel two-photon-absorbing (2PA) materials, which can be excited by near-infrared (NIR) light (700−1100 nm), is an area of intensive research because of their potential applications for frequency up-conversion lasing, high-density optical storage, holographic data storage, 3-D microfabrication, two-photon fluorescence microscopy, and photodynamic therapy.[1] Environmental sensing materials based on 2PA materials for detecting various metal ions, the fluoride ion, and pH values have been reported recently.[2–6] 2PA sensing materials with two-photon fluorescence (2PF) have many advantages over the commonly used one-photon fluorescence (1PF) materials (excited with the light in the range 300−600 nm in wavelength). These include exclusive confinement of the excitation to the focal volume with high 3D resolution and reduced photobleaching and phototoxicity by virtue of the low-energy NIR excitation with greater depths of penetration in living tissues for biological applications.[7] Although the advantages of using 2PA sensing materials are clear, only a few 2PA metal ion sensors have been reported.[2,3,6] The selectivity and sensitivity demonstrated in these sensing materials still need to be improved.

The selective detection of zinc ion is extremely important in environmental or biological systems.[8] Various 1PF-based sensing materials for Zn^{2+}, including fluorescein, quinoline, and 2-(2′-hydroxyphenyl)benzoxazole (HPBO) derivatives, have been developed for this purpose.[9,10] However, investigation on the 2PF-based zinc sensor is quite limited.[6]

The HPBO-based functional materials can undergo excited-state intramolecular proton transfer (ESIPT, as shown in

* To whom all correspondence should be addressed. Tel: (206)543-2626; Fax: (206)543-3100; E-mail: ajen@u.washington.edu.
† Department of Materials Science and Engineering, University of Washington.
‡ Department of Chemical Engineering, National Taiwan University.
§ Institute of Advanced Materials and Technology, University of Washington.
|| Institute of Polymer Science and Engineering, National Taiwan University.

(1) See a recent review: Lin, T. C.; Chung, S. J.; Kim, K. S.; Wang, X. P.; He, G. S.; Swiatkiewica, J.; Pudavar, H. E.; Prasad, P. N. In *Advances in Polymer Science*; Lee K. S., Ed.; Springer: Berlin, 2003; Vol. 161; p 157.
(2) Pond, S. J. K.; Tsutsumi, O.; Rumi, M.; Kwon, O.; Zojer, E.; Brédas, J. L.; Marder, S. R.; Perry, J. W. *J. Am. Chem. Soc.* **2004**, *126*, 9291.
(3) (a) Kim, K. M.; Jeong, M. Y.; Ahn, H. C.; Jeon, S. J.; Cho, B. R. *J. Org. Chem.* **2004**, *69*, 5749. (b) Ahn, H. C.; Yang, S. K.; Kim, H. M.; Li, S. J.; Jeon, S. J.; Cho, B. R. *Chem. Phys. Lett.* **2005**, *410*, 312. (c) Kim, J. S.; Kim, H. J.; Kim, H. M.; Kim, S. H.; Lee, J. W.; Kim, S. K.; Cho, B. R. *J. Org. Chem.* **2006**, *71*, 8016. (d) Kim, H. M.; Yang, P. Y.; Seo, M. S.; Yi, J.-S.; Hong, J. H.; Jeon, S.-J.; Ko, Y.-G.; Lee, K. J.; Cho, B. C. *J. Org. Chem.* **2007**, *72*, 2088.
(4) Werts, M. H. V.; Gmouh, S.; Mongin, O.; Pons, T.; Blanchard-Desce, M. *J. Am. Chem. Soc.* **2004**, *126*, 16294.
(5) (a) Liu, Z. Q.; Shi, M.; Li, F. Y.; Fang, Q.; Chen, Z. H.; Yi, T.; Huang, C. *Org. Lett.* **2005**, *7*, 5481. (b) Zhang, M.; Li, M.; Zhao, Q.; Li, F.; Zhang, D.; Zhang, J.; Yia, T.; Huang, C. *Tetrahedron Lett.* **2007**, *48*, 2329.
(6) Bozio, R.; Cecchetto, E.; Fabbrini, G.; Ferrante, C.; Maggini, M.; Menna, E.; Pedron, D.; Ricco, R.; Signorini, R.; Zerbetto, M. *J. Phys. Chem. A* **2006**, *110*, 6459.
(7) Cahalan, M. D.; Parker, I.; Wei, S. H.; Miller, M. J. *Nat. Rev. Immunol.* **2002**, *2*, 872.

10.1021/cm702527m CCC: $40.75
Published on Web 01/25/2008

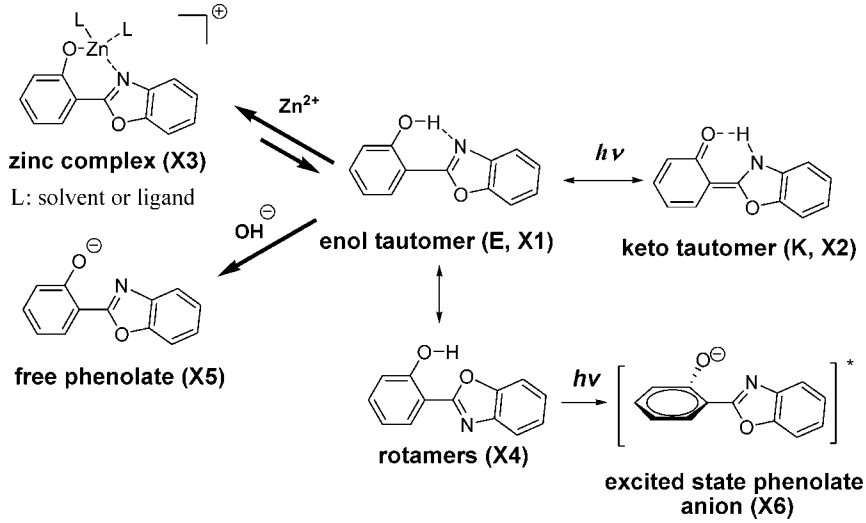

Figure 1. Chemical structures related with tautomer, rotamer, complex, and phenolate ion of the HPBO moiety.

Figure 1) by the structural transformation between the enol (X1) and keto tautomers (X2).[11] The ESIPT of the HPBO could result in a large Stokes shift ranging from 100 to 500 nm. Furthermore, the HPBO moiety can also chelate with the zinc ions (X3). And during the process of the coordination with zinc ion, the phenol group in the HPBO is deprotonated, and the generated phenolate anion acts as a donor in the zinc complex (Figure 1).[10a−c] Through the complexation with zinc ions, the ESIPT process is efficiently disrupted, and a blue-shifted emission is detected from the zinc complex.[10c] On the other hand, under basic conditions, the phenol group of the HPBO moiety could be easily deprotonated to form a free phenolate anion (X5)[12] (the HPBO moiety with the free phenolate anion is called phenolated HPBO), resulting in the disruption of the ESIPT.

Because of these specific characteristics, HPBO-containing materials are considered to be a promising class of functional materials for sensors[10] (including zinc ion sensors[10a−c] and pH sensors[10c,d]), light-emitting diodes,[13] and photolithography.[14] Although many HPBO derivatives have been investigated so far,[10,11,13–15] to the best of our knowledge, metal ions and pH sensors based on 2PA chromophores with HPBO groups have never been reported. Herein, we report a series of new 2PA HPBO-containing chromophores as zinc ion and pH sensors by modulating the ESIPT properties of the HPBO groups via metal complex formation and base stimulation.

The chemical structures of the novel 2PA chromophores (**1**, **2**, and **3**) shown in Figure 2 have the fluorene vinylene moiety in the structural center and HPBO derivatives as the end group. The new 2PA chromophores have the same conjugation length but different donor end groups (OH and

(8) (a) Vallee, B. L.; Falchuk, K. H. *Physiol. Rev* **1993**, *73*, 79. (b) Lippard, S. J.; Berg, J. M. *Principles of Bioinorganic Chemistry*; University Science Books: Mill Valley, 1994. (c) Berg, J. M.; Shi, Y. G. *Science* **1996**, *271*, 1081. (d) Roat-Malone, R. M. *Bioinorganic Chemistry: A Short Course*; John Wiley & Sons: New York, 2002. (e) Sorensen, M. B.; Stoltenberg, M.; Juhl, S.; Danscher, G.; Ernst, E. *Prostate* **1997**, *31*, 125. (f) Gee, K. R.; Zhou, Z. L.; Qian, W. J.; Kennedy, R. *J. Am. Chem. Soc.* **2002**, *124*, 776. (g) Danscher, G. *Histochemistry* **1981**, *71*, 81. (h) Frederickson, C. J.; Suh, S.; Silva, D.; Thompson, R. B. *J. Nutr.* **2000**, *130*, 1471S. (i) Kay, A. R. *J. Neurosci.* **2003**, *23*, 6847. (j) Bush, A. I. *Curr. Opin. Chem. Biol.* **2000**, *4*, 184.

(9) (a) Lim, N. C.; Freake, H. C.; Brückner, C. *Chem.—Eur. J.* **2005**, *11*, 38. (b) Chang, C. J.; Nolan, E. M.; Jaworski, J.; Okamoto, K.; Hayashi, Y.; Sheng, M.; Lippard, S. J. *Inorg. Chem.* **2004**, *43*, 6774. (c) Chang, C. J.; Jaworski, J.; Nolan, E. M.; Sheng, M.; Lippard, S. J. *Proc. Natl. Acad. Sci. U.S.A.* **2004**, *101*, 1129. (d) Hirano, T.; Kikuchi, K.; Urano, Y.; Higuchi, T.; Nagano, T. *J. Am. Chem. Soc.* **2000**, *122*, 12399. (e) Hirano, T.; Kikuchi, K.; Urano, Y.; Nagano, T. *J. Am. Chem. Soc.* **2002**, *124*, 6555. (f) Komatsu, K.; Kikuchi, K.; Kojima, H.; Urano, Y.; Nagano, T. *J. Am. Chem. Soc.* **2005**, *127*, 10197. (g) Frederickson, C. J.; Kasarskis, E. J.; Ringo, D.; Frederickson, R. E. *J. Neurosci. Methods* **1987**, *20*, 91. (h) Zalewski, P. D.; Forbes, I. J.; Betts, W. H. *Biochem. J.* **1993**, *296*, 403.

(10) (a) Taki, M.; Wolford, J. L.; O'Halloran, T. V. *J. Am. Chem. Soc.* **2004**, *126*, 712. (b) Lim, H. N. C.; Freake, N. C.; Brückner, C. *Chem.—Eur. J.* **2005**, *11*, 38. (c) Henary, M. M.; Fahrni, C. J. *J. Phys. Chem. A* **2002**, *106*, 5210. (d) Tanaka, K.; Kumagi, T.; Aoki, H.; Deguchi, M.; Iwata, S. *J. Org. Chem.* **2001**, *66*, 7328. (e) Lee, J. K.; Lee, T. S. *J. Polym. Sci., Part A: Polym. Chem.* **2005**, *43*, 1397. (f) Tong, H.; Zhou, G.; Wang, L. X.; Jing, X. B.; Wang, F. S.; Zhang, J. P. *Tetrahedron Lett.* **2003**, *44*, 131. (g) Lee, J. K.; Na, J. H.; Park, W. H.; Lee, T. S.; Kwon, Y. K. *Mol. Cryst. Liq. Cryst.* **2004**, *424*, 245. (h) Ohshima, A.; Momotake, A.; Arai, T. *Tetrahedron Lett.* **2004**, *45*, 9377. (i) Yang, C.-C.; Tian, Y.; Chen, C.-Y.; Jen, A. K.-Y.; Chen, W.-C. *Macromol. Rapid Commun.* **2007**, *28*, 894.

(11) (a) Kozich, V.; Dreyer, J.; Vodchits, A.; Werncke, W. *Chem. Phys. Lett.* **2005**, *415*, 121. (b) Ikegami, M.; Arai, T. *Chem. Lett.* **2000**, 996. (c) Das, K.; Sarkar, N.; Gsosh, A. K.; Majumdar, D.; Nath, D. N.; Bhattacharyya, K. *J. Phys. Chem.* **1994**, *98*, 9126. (d) Abou-Zied, O. K.; Jimenez, R.; Thompson, E. H. Z.; Millar, D. P.; Romesberg, F. E. *J. Phys. Chem. A* **2002**, *106*, 3665. (e) Seo, J.; Kim, S. H.; Park, S. Y. *J. Am. Chem. Soc.* **2004**, *126*, 11154. (f) Ernsting, N. P.; Kovalenko, S. A.; Senyushkina, T.; Saam, J.; Farztdinov, V. *J. Phys. Chem. A* **2001**, *105*, 3443. (g) Tanaka, K.; Deguchi, M.; Yamaguchi, K.; Yamada, K.; Iwata, S. *J. Heterocycl. Chem.* **2001**, *38*, 131. (h) Potter, C. A. S.; Brown, R. G. *Chem. Phys. Lett.* **1988**, *153*, 7. (i) Elsaesser, T.; Schmetzer, B. *Chem. Phys. Lett.* **1987**, *140*, 293. (j) Potter, C. A. S.; Brown, R. G.; Vollmer, F.; Rettig, W. *J. Chem. Soc., Faraday Trans.* **1994**, *90*, 59. (k) Stryukov, M. B.; Lyubarkaya, A. E.; Knyazhanskii, M. I. *Zh. Prikl. Specktrosk.* **1977**, *27*, 1055.

(12) It should be noted that there might be a torsion angle between the phenolate group and benzoxazole unit. We did not calculate this torsion angle. For simplification, there is no torsion angle described in the X5-containing structures.

(13) (a) Kim, Y. K.; Lee, J. G.; Kim, S. *Adv. Mater.* **1999**, *11*, 1463. (b) Kim, Y. K.; Oh, E. S.; Choi, D. K.; Lim, H. T.; Ha, C. S. *Nanotechnology* **2004**, *15*, 149. (c) Yasuda, T.; Yamaguchi, Y.; Fujita, K.; Tsutsui, T. *Chem. Lett.* **2003**, *32*, 644.

(14) (a) Park, S. H.; Kim, S. H.; Seo, J. W.; Park, S. Y. *Macromolecules* **2005**, *38*, 4557. (b) Lee, J. K.; Kim, H. J.; Kim, T. H.; Lee, C. H.; Park, W. H.; Kim, J.; Lee, T. S. *Macromolecules* **2005**, *38*, 9427. (c) Tangirala, R.; Baer, E.; Hitner, A.; Weder, C. *Adv. Funct. Mater.* **2004**, *14*, 596.

(15) (a) Dupradeau, F. Y.; Case, D. A.; Yu, C. Z.; Jimenez, R.; Romesberg, F. E. *J. Am. Chem. Soc.* **2005**, *127*, 15612. (b) Ogawa, A. K.; Abou-Zied, O. K.; Tsui, V.; Jimenez, R.; Case, D. A.; Romesberg, F. E. *J. Am. Chem. Soc.* **2000**, *122*, 9917. (c) Wang, H.; Zhang, H.; Abou-Zied, O. K.; Yu, C.; Romesberg, F. E.; Glasbeek, M. *Chem. Phys. Lett.* **2003**, *367*, 599.

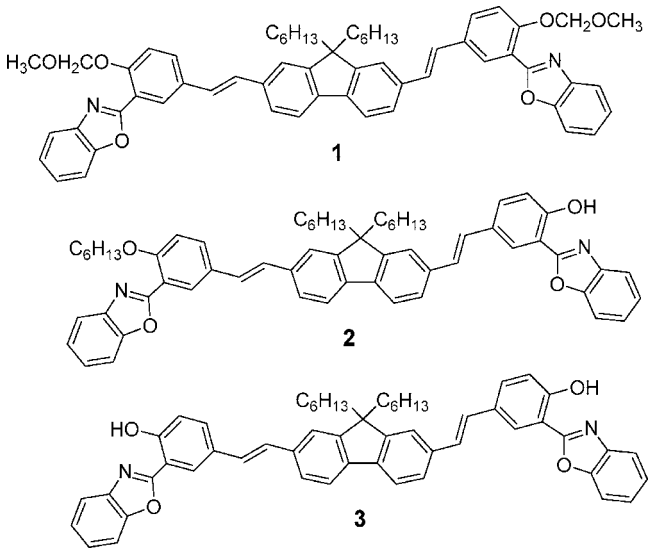

Figure 2. Chemical structures of the new HPBO derivatives, **1**, **2**, and **3**.

OCH_2R, where R = OCH_3 for **1** and C_5H_{11} for **2**). Therefore, the materials reported here are a series of compounds which could provide the systematic correlations among the chemical structures, selectivity, and sensitivity for ions and 1PF/2PF properties.

2. Experimental Section

2.1. Materials. 2,7-Dibromo-9,9-dihexylfluorene (**4**), methyltriphenylphosphonium bromide, sodium hydride, 2-aminophenol, chloromethyl methyl ether, diisopropylethylamine, tributylvinyltin, 1-bromohexane, tributylamine, palladium acetate, tri(*o*-tolyl)phosphine, $Zn(OOCCH_3)_2$, $Zn(ClO_4)_2$, $ZnCl_2$, $Mg(ClO_4)_2$, $KOOCCH_3$, $NaOOCCH_3$, LiCl, $Ca(OOCCH_3)_2$, $Fe(NO_3)_3 \cdot H_2O$, $Cu(OOCCH_3)_2 \cdot H_2O$, and $NiCl_2$ were used as received from Aldrich. 2,7-Diformyl-9,9-di-*n*-hexylfluorene (**5**) and 2,7-divinyl-9,9-di-*n*-hexylfluorene (**6**) were prepared according to previously described procedures.[16]

2.2. Synthesis. The chromophores were synthesized by using common organic reactions including the Heck reaction,[17] Wittig reaction,[18] and Stille coupling, [19] as shown in Schemes 1 and 2.

2.2.1. Synthesis of 1 and 3. *2-Benzoxazol-2-yl-4-bromophenol (**8**).* 5-Bromo-2-hydroxybenzaldehyde (**7**, 1.50 g, 8.0 mmol) and 2-aminophenol (1.92 g, 9.6 mmol) were added to 40 mL of acetic acid. After stirring for 10 min at room temperature, lead(IV) acetate (3.89 g, 8.8 mmol) was added to the mixture. The reaction mixture was stirred for 30 min and then gently boiled at 110 °C for an additional 30 min. The mixture was cooled down, poured into cold water, and neutralized with aqueous NaOH solution. The precipitate was filtered, extracted in ethyl acetate, and dried with $MgSO_4$. After the solvent was removed, the crude product was purified by using silica gel column chromatography with hexane/methylene chloride (5/1 by volume) as an eluent to afford 0.72 g of white powder with a yield of 25%; mp 174−176 °C. R_f (hexane/methylene chloride, 5/1 by volume): 0.33. ^{1}H NMR (300 MHz, $CDCl_3$, 25 °C, TMS): δ = 11.46 (s, 1H), 8.18 (s, 1H), 7.78 (m, 1H), 7.64 (m, 1H), 7.56 (dd, J = 9 Hz, 1H,), 7.45 (m, 2H), 7.03 (dd, 1H, J = 9 Hz).^{13}C NMR (125 MHz, $CDCl_3$, 25 °C): δ =161.8, 157.9, 149.4, 140.0, 136.4, 129.6, 126.1, 125.5, 119.7, 119.6, 112.4, 111.6, 111.0.

*2-(5-Bromo-2-methoxymethoxyphenyl)benzoxazole (**9**).* **8** (1.6 g, 5.5 mmol) and diisopropylethylamine (13.5 mL, 27.6 mmol) were dissolved in CH_2Cl_2 (20 mL), and the mixture was cooled to 0 °C in an ice bath. Chloromethyl methyl ether (2.1 mL, 19.7 mmol) was added to the mixture. The reaction was kept at room temperature for 12 h, then washed with 5% $NaHCO_3$ aqueous solution, and dried over $MgSO_4$. After the solvent was removed, the crude product was purified by column chromatography using hexane/methylene chloride (5:1 by volume) as the eluent to afford a white powder of 1.8 g with the yield of 98%. R_f (methylene chloride): 0.49. ^{1}H NMR (300 MHz, $CDCl_3$, 25 °C, TMS): δ = 8.29 (s, 1H), 7.78 (d, J = 7 Hz, 1H), 7.61 (m, 2H), 7.40 (d, J = 7 Hz, 2H), 7.23 (m, 1H), 5.35 (s, 2H), 3.54 (s, 3H). ^{13}C NMR (125 MHz, $CDCl_3$, 25 °C): δ =160.4, 155.3, 150.8, 142.0, 135.3, 133.9, 125.5, 124.7, 120.5, 119.5, 118.5, 114.6, 110.8, 95.5, 56.7.

*3,3′-Bis(2-benzoxazol-2-yl)-(4,4′-[(9,9-dihexylfluorene-2,7-diyl)di-(1*E*)-2,1-ethenediyl]bisphenol (**3**).* **9** (0.30 g, 0.91 mmol), **6** (0.16 g, 0.41 mmol), $Pd(OAc)_2$ (4.5 mg, 0.02 mmol), and tri-*o*-tolylphosphine (31.0 mg, 0.01 mmol) were dissolved in 6 mL of a DMF/$(C_4H_9)_3N$ mixture (12:1 by volume). The mixture was degassed with N_2 for 15 min and then heated at 130 °C for 16 h. After cooling down, the mixture was poured into water and extracted with ethyl acetate. The organic layer was washed with water and brine and dried over Na_2SO_4. After the solvent was removed, the residue was purified by column chromatography using hexane/ethyl acetate (20:1 by volume) as an eluent to afford 0.16 g of yellow solid with the yield of 49%; mp 181−183 °C. R_f (hexane/ethyl acetate, 20/1 by volume): 0.11. ^{1}H NMR (300 MHz, $CDCl_3$, 25 °C, TMS): δ = 11.50 (s, 2H), 8.20 (s, 2H), 7.75 (m, 2H), 7.66 (m, 6H), 7.52 (m, 4H), 7.42 (m, 4H), 7.16 (m, 4H), 7.14 (d, J = 9 Hz, 2H), 2.04 (m, 4H), 1.11 (m, 12H), 0.79 (t and m, 10H). ^{13}C NMR (125 MHz, $CDCl_3$, 25 °C, TMS): δ =158.3, 151.6, 149.2, 140.6, 140.1, 136.3, 131.5, 129.6, 128.2, 126.7, 125.5, 125.1, 125.0, 120.7, 119.9, 119.3, 117.9, 110.7, 110.6, 55.0, 40.7, 31.6, 29.8, 23.9, 22.6, 14.0. EI-HRMS *m/e* calculated for $C_{55}H_{53}N_2O_4$ (M + H) 805.4005; found 805.4018.

*3,3′-Bis(2-benzoxazol-2-yl)-(4,4′-[(9,9-dihexyl-fluorene-2,7-diyl)di-(1*E*)-2,1-ethenediyl]bisphenyl Methoxymethyl Ether (**1**).* **3** (40 mg, 0.05 mmol) and diisopropylethylamine (0.14 mL, 0.28 mmol) were dissolved in CH_2Cl_2 (5 mL), and the mixture was cooled to 0 °C in an ice bath. Chloromethyl methyl ether (0.2 mL, 2 mmol) was added into the mixture. The reaction was kept at room temperature for 12 h, then washed with 5% $NaHCO_3$ aqueous solution, and dried over $MgSO_4$. After the solvent was removed, the crude product was purified by column chromatography using hexane/methylene chloride (5:1 by volume) as an eluent to afford a pale yellow powder of 38 mg with the yield of 85%. R_f (CH_2Cl_2): 0.38. ^{1}H NMR (300 MHz, $CDCl_3$, 25 °C, TMS): 8.37 (s, 2H), 7.84 (m, 2H), 7.68 (m, 6H), 7.55 (m, 4H), 7.45 (m, 4H), 7.34 (d, 2H, J = 9.0 Hz), 7.24 (m, 4H), 5.42 (s, 4H), 3.60 (s, 6H), 2.04 (m, 4H), 1.14 (m, 12H), 0.76 (t and m, 10H). ^{13}C NMR (125 MHz, $CDCl_3$, 25 °C, TMS): δ =161.9, 155.6, 151.8, 150.9, 142.2, 140.9, 136.4, 132.1, 130.6, 129.4, 129.3, 126.5, 125.8, 125.3, 124.6, 120.9, 120.4, 120.2, 118.0, 117.1, 110.8, 95.5, 56.7, 55.2, 40.8, 31.7, 30.0, 24.0, 22.8, 14.2. EI-HRMS *m/e* calculated for $C_{59}H_{61}N_2O_6$ (M + H) 893.4530; found 893.4524.

(16) (a) See the two recent reviews: Li, C. J. *Chem. Rev.* **2005**, *105*, 3095. (b) Nicolaou, K. C.; Bulger, P. G.; Sarlah, D. *Angew. Chem., Int. Ed.* **2005**, *44*, 4442.
(17) See a recent review: Bell, A. D.; Edmonds, M. K. *Organophosphorus Reagents* **2004**, 99.
(18) See a recent review: Dounay, A. B.; Overman, L. E. *Chem. Rev.* **2003**, *103*, 2945.
(19) Wang, W. L.; Xu, J. W.; Lai, Y. H.; Wang, F. K. *Macromolecules* **2004**, *37*, 3546.
(20) Hamai, S.; Hirayama, F. *J. Phys. Chem.* **1983**, *87*, 83.

Scheme 1

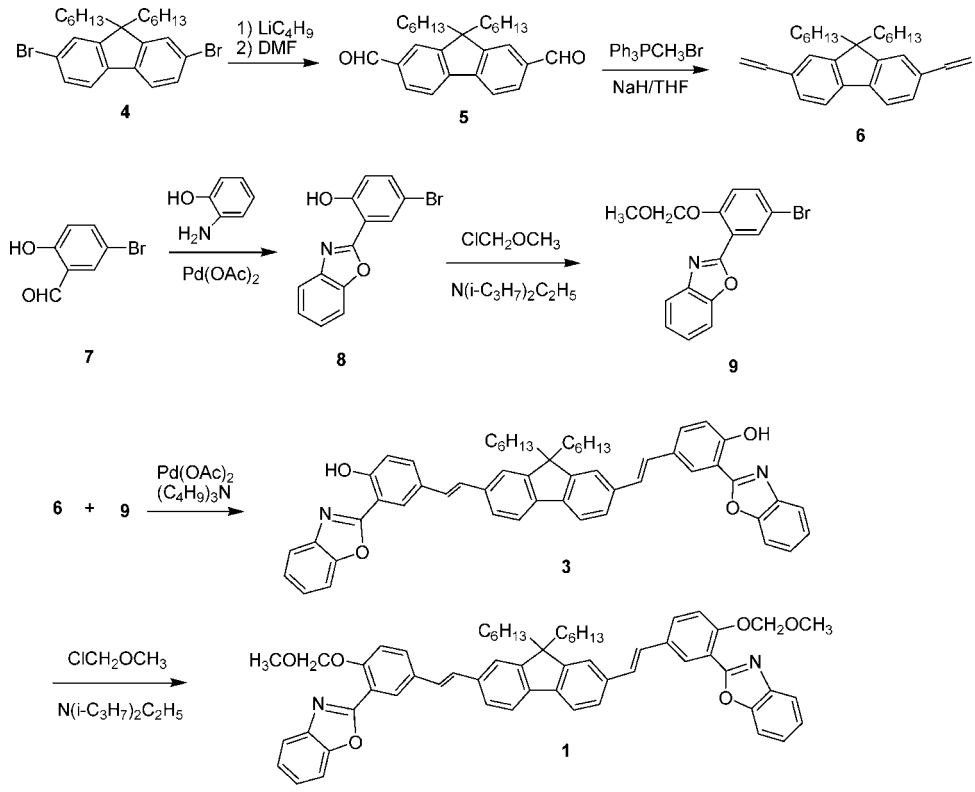

Scheme 2

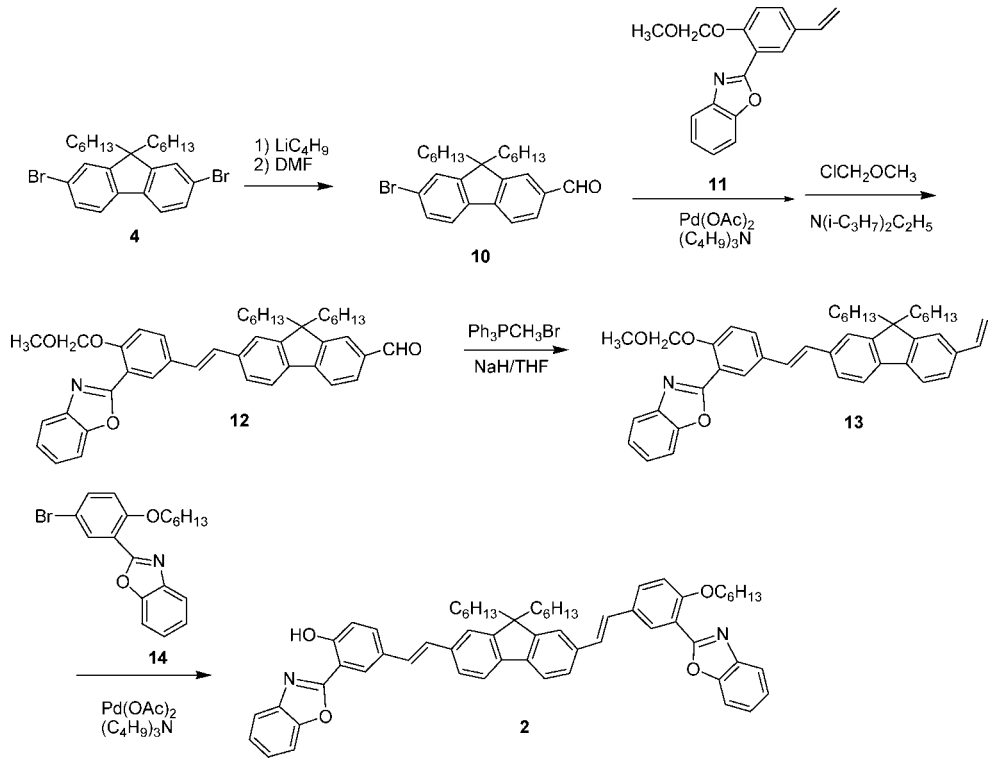

2.3.2. Synthesis of 2. *2-Formyl-7-bromo-9,9-dihexylfluorene (**10**).* 8.0 g (16 mmol) of compound **4**was dissolved into 200 mL of dry ether and cooled to –78 °C under stirring. *n*-Butyllithium (8.2 mL, 2.5 M) in hexane (20 mmol) was added into the solution. The solution was warmed to room temperature for 30 min and then cooled down to –78 °C. DMF (6 mL, 70 mmol) was added into the mixture. The mixture was then warmed to room temperature and kept under stirring for 16 h. The mixture was poured in to 200 mL of water; the organic layer was separated and dried over Na_2SO_4. The solvent was removed, and the residue was purified through column chromatography with hexane/ethyl acetate (10:1 by volume). A colorless oil with the yield of 70% (5.0 g) was obtained. The oil solidified after standing at room temperature for 3 days. R_f (hexane/ethyl acetate, 10/1 by volume): 0.14. ^{1}H NMR

(300 MHz, $CDCl_3$, 25 °C, TMS): 10.08 (s, 1H), 7.88 (s and d, 3H), 7.64 (d, $J = 7.8$ Hz, 1H), 7.53 (s and d, 2H), 2.04 (m, 4H), 1.22 (m, 12H), 0.82 (t, $J = 7.2$ Hz, 6H), 0.58 (m, 4H). ^{13}C NMR (125 MHz, $CDCl_3$, 25 °C): δ =192.4, 154.4, 151.3, 146.5, 138.7, 135.7, 130.8, 130.6, 126.6, 123.3, 123.2, 122.4, 120.3, 55.7, 40.3, 31.6, 29.7, 23.8, 22.7, 14.2. MS (EI): 441.3 (M^+), 442.3 ($M^+ + 1$), 443.2 ($M^+ + 2$), 444.2 ($M^+ + 3$).

*2-(2-Methoxymethoxyphenyl-5-vinyl)benzoxazole (**11**).* **9** (300 mg, 0.90 mmol), tributylvinyltin (400 mg, 1.2 mmol), and tetrakis (triphenylphosphine)palladium(0) (40 mg, 0.034 mmol) were dissolved in toluene (5 mL) and heated at refluxing under nitrogen for 16 h. The mixture was cooled down, and then the solvent was removed under reduced pressure. The residue was passed through a column chromatography with hexane/ethyl acetate (10:1 by volume) to produce 170 mg of a white solid with the yield of 67%. R_f (hexane/ethyl acetate, 3/1 by volume): 0.40. ^{1}H NMR (300 MHz, $CDCl_3$, 25 °C, TMS): 8.18 (s, 1H), 7.84 (m, 1H), 7.62 (m, 1H), 7.57 (dd, $J = 7.8$ Hz, 1H), 7.38 (m, 2H), 7.30 (s, 1H), 6.77 (m, 1H), 5.78 (d, $J = 17.1$ Hz, 1H), 5.37 (s, 2H), 5.28 (d, $J = 10.8$ Hz, 1H), 3.56 (s, 3H). ^{13}C NMR (125 MHz, $CDCl_3$, 25 °C): δ = 161.7, 155.7, 150.8, 142.1, 135.4, 132.0, 130.2, 129.3, 125.2, 124.5, 120.3, 117.7, 116.8, 113.8, 110.7, 95.3, 56.6. MS (EI): 282.4 (M^+).

*2-Formyl-7-{2-[3-(benzoxazol-2-yl)-4-methoxymethoxyphenyl]-vinyl}-9,9-dihexylfluorene (**12**).* **10** (1.7 g, 3.9 mmol), **11** (1.1 g, 3.9 mmol), palladium acetate (24 mg, 0.10 mmol), tri-*o*-tolylphosphine (120 mg, 0.39 mmol), and tributylamine (4 mL) were dissolved in DMF (20 mL) and heated at 130 °C for 24 h under nitrogen. The mixture was cooled down and poured into 300 mL of water. The organic materials were extracted into ethyl acetate and dried over Na_2SO_4. After the solvent was removed under vacuum, the residue was dissolved in 30 mL of dry methylene chloride. Diisopropylethylamine (2.8 mL, 5.6 mmol) and chloromethyl methyl ether (0.6 mL, 6 mmol) were added to the mixture. The reaction was kept at room temperature for 12 h, then was washed with 5% $NaHCO_3$ aqueous solution, and dried over $MgSO_4$. After the solvent was removed, the crude product was purified by column chromatography using hexane/methylene chloride (5:1 by volume) as eluent to afford a yellow powder of 1.2 g with the yield of 50%. R_f (methylene chloride): 0.33. ^{1}H NMR (300 MHz, $CDCl_3$, 25 °C, TMS): 10.08 (s, 1H), 8.27 (s, 1H), 7.87 (m, 4H), 7.67 (m, 4H), 7.41 (m, 4H), 7.25 (m, 2H), 5.42 (s, 2H), 3.59 (s, 3H), 2.04 (m, 4H), 1.07 (m, 12H), 0.78 (t, $J = 6.6$ Hz, 6H), 0.72 (m, 4H). ^{13}C NMR (125 MHz, $CDCl_3$, 25 °C) δ = 192.5, 161.8, 155.7, 153.0, 151.9, 150.8, 147.4, 142.1, 139.4, 138.1, 135.4, 131.7, 130.8, 130.6, 129.5, 128.8, 127.6, 126.0, 125.2, 124.6, 123.2, 121.4, 121.1, 120.3, 120.1, 118.0, 117.0, 110.7, 95.4, 56.7, 55.4, 40.4, 31.6, 29.8, 23.9, 22.7, 14.1. MS (EI): 642.6 ($M^+ + 1$).

*2-Vinyl-7-{2-[3-(benzoxazol-2-yl)-4-methoxymethoxyphenyl]-vinyl}-9,9-dihexylfluorene (**13**).* **12** (1.2 g, 1.9 mmol) and methyltriphenylphosphonium bromide (1.0 g, 2.82 mmol) were suspended in dry THF (50 mL), and NaH (100 mg, 4.2 mmol) was added into the mixture. The mixture was stirred at room temperature under nitrogen overnight, and then 100 mL of water was added into the mixture. The organic layer was extracted with ethyl acetate and dried over Na_2SO_4. The solvent was removed, and the residue was purified through column chromatography with hexane/ethyl acetate (20:1 by volume). 0.80 g of yellow solid was obtained. Yield: 67%. R_f (hexane/ethyl acetate, 20/1 by volume): 0.08. Yield: 67%. ^{1}H NMR (300 MHz, $CDCl_3$, 25 °C, TMS): 8.36 (s, 1H), 7.86 (m, 1H), 7.68 (m, 3H), 7.54 (m, 1H), 7.40 (m, 8H), 7.22 (s, 1H), 6.88 (m, 1H), 5.84 (d, $J = 17.5$ Hz, 1H), 5.42 (s, 2H), 5.29 (d, $J = 10.8$ Hz, 1H), 3.59 (s, 3H), 2.04 (m, 4H), 1.07 (m, 12H), 0.78 (t, $J = 7.2$ Hz, 6H), 0.72 (m, 4H). ^{13}C NMR (125 MHz, $CDCl_3$, 25 °C): δ = 161.8, 155.5, 151.7, 151.6, 150.8, 142.1, 140.9, 140.8, 137.6, 136.7, 136.3, 132.1, 130.5, 129.4, 129.3, 126.4, 125.7, 125.5, 125.2, 124.6, 120.9, 120.7, 120.4, 120.1, 119.9, 117.9, 117.0, 113.2, 110.7, 95.4, 56.7, 55.1, 40.7, 31.7, 29.9, 23.9, 22.8, 14.2. MS (EI): 640.9 ($M^+ + 1$).

*2-(5-Bromo-2-hexyloxyphenyl)benzoxazole (**14**).* Compound **8** (580 mg, 2 mmol), 1-bromohexane (400 mg, 2.4 mmol), potassium carbonate (276 mg, 2 mmol), and potassium iodide (100 mg) were suspended in acetone (10 mL) and heated at refluxing for 16 h. The solid was filtered off, and the solvent was removed. The residue was passed through column chromatography with hexane/ethyl acetate (20:1 by volume) as the eluent to produce 380 mg of product with the yield of 51%. R_f (hexane/ethyl acetate, 5/1 by volume): 0.44. ^{1}H NMR (300 MHz, $CDCl_3$, 25 °C, TMS): 8.28 (s, 1H), 7.77 (m, 1H), 7.58 (m, 2H), 7.36 (m, 2H), 6.92 (d, $J = 9.0$ Hz, 1H), 4.12 (t, 2H), 1.96 (m, 2H), 1.62 (m, 2H), 1.20 (m, 4H), 0.96 (t, $J = 6.6$ Hz, 3H). ^{13}C NMR (125 MHz, $CDCl_3$, 25 °C): δ =160.9, 157.2, 150.8, 141.8, 135.3, 133.8, 125.3, 124.6, 120.2, 118.3, 115.0, 112.7, 110.6, 69.5, 31.6, 29.1, 25.7, 22.8, 14.2. MS (EI): 374.2 (M^+), 375.1 ($M^+ + 1$), 376.1 ($M^+ + 2$).

*3,3′-Bis(2-benzoxazol-2-yl)-(4,4′-[(9,9-dihexylfluorene-2,7-diyl)di-(1E)-2,1-ethenediyl]bisphenol Monohexyl Ether (**2**).* **14** (75 mg, 0.2 mmol), **13** (150 mg, 0.24 mmol), palladium acetate (4 mg, 0.016 mmol), tri-*o*-tolylphosphine (20 mg, 0.065 mmol), and tributylamine (0.4 mL) were dissolved in DMF (5 mL) and heated at 130 °C for 24 h under nitrogen. The mixture was cooled down and poured into water (50 mL), and the organic materials were extracted into ethyl acetate and dried over Na_2SO_4. After the solvent was removed under vacuum, the residue was purified by column chromatography using hexane/methylene chloride (20:1 by volume) as the eluent to afford a yellow solid of 80 mg with the yield of 45%; mp 75 °C. R_f (hexane/methylene chloride, 5/1 by volume): 0.12. ^{1}H NMR (300 MHz, $CDCl_3$, 25 °C, TMS): 11.58 (s, 1H), 8.38 (s, 1H), 8.24 (s, 1H), 7.85 (m, 1H), 7.79 (m, 1H), 7.67 (m, 6H), 7.55 (m, 4H), 7.38 (m, 4H), 7.22 (m, 4H), 7.11 (m, 2H), 4.20 (t, 2H), 2.07 (m, 4H), 1.91 (m, 2H), 1.62 (m, 2H), 1.11 (m, 16H), 0.96 (t, 3H), 0.78 (t, 6H), 0.72 (m, 4H). ^{13}C NMR (125 MHz, $CDCl_3$, 25 °C, TMS): δ 162.8, 162.3, 158.3, 157.5, 151.7, 151.5, 150.8, 149.2, 141.9, 140.6, 140.5, 140.0, 135.4, 135.3, 131.5, 130.6, 130.4, 129.6, 129.4, 127.5, 127.2, 125.7, 125.5, 125.6, 125.5, 125.1, 125.0, 124.9, 124.4, 120.7, 120.6, 120.0, 119.9, 119.3, 117.9, 116.8, 113.7, 110.7, 110.6, 110.5, 69.3, 55.0, 40.7, 31.6, 29.9, 29.8, 29.2, 25.7, 23.9, 22.7, 14.1, 14.1. EI-HRMS *m/e* calculated for $C_{61}H_{65}N_2O_4$ (M + H) 889.4944; found 889.4958.

2.3. Characterizations. *2.3.1. General Information.* ^{1}H NMR spectra were measured using a Bruker 300 instrument spectrometer operating at 300 MHz with TMS internal standard as a reference for chemical shifts. ^{13}C NMR spectra were measured using a Bruker 500 instrument spectrometer operating at 125 MHz. High-resolution mass spectrometry (HRMS) was performed by the UW Bio Mass Spectrometry Laboratory. Thermal transitions were measured on a TA Instruments differential scanning calorimeter (DSC) 2010 with heating and cooling rates of 10 °C min^{-1}. UV–vis spectra were recorded with a Hewlett-Packard 8452A diode array UV–vis spectrophotometer. One-photon fluorescence spectra were recorded with a Perkin-Elmer luminescence spectrometer LS 50B using a xenon lamp as a light source with the emission and excitation slit of 5 nm. The silica gel for column chromatography was purchased from MP SiliTech (Solon, OH) with a 60 Å mean pore size and particle size of 32–63 μm. Baker-flex silica gel IB2-F (Krackeler Scientific Inc., New York) with a thickness of 0.25 mm was used for thin layer chromatography (TLC) analysis. Dimethylformamide (DMF) (UV–vis spectroscopy grade) was purchased from Aldrich. All

of the solutions were prepared in air.

2.3.2. Determination of Quantum Yields. Fluorescence quantum yield measurement was carried out on a Perkin-Elmer LS 50B luminescence spectrometer. The fluorescence quantum yields of samples (s) in solutions were recorded by using 9,10-diphenylanthracene ($\eta = 0.90$)[20] excited at 390 nm. η was calculated according to the following equation:[21]

$$\eta_s = \eta_r\left(\frac{A_r}{A_s}\right)\left(\frac{I_s}{I_r}\right)\left(\frac{n_s^2}{n_r^2}\right) \quad (1)$$

where η_r and η_s are the respective fluorescence quantum yields of standard and samples, A_r and A_s are the respective absorbances of standard and the measured samples at the excitation wavelength, I_r and I_s are the respective integrated emission intensities of standards and the samples, and n_r and n_s are the respective refractive indices of the corresponding solvents of the solutions. The quantum yields were measured using three different concentrations. Optical densities of all of the solutions at the excitation wavelength were set about 0.03, 0.05, and 0.08. An error of $\pm 10\%$ is estimated for the fluorescence quantum yield measurement.

2.3.3. Determination of Two-Photon Cross Sections. Two-photon excitation spectra were measured using a two-photon induced fluorescence technique[22] using a mode-locked Ti:sapphire laser excitation source (Coherent, Mira 900). The laser provides a pulse of ~160 fs pulse width at a pulse repetition frequency of 76 MHz in the wavelength range of 710−1000 nm. The pumping wavelengths were determined by a monochromator−CCD system. Fluorescein in basic water (pH 11), which has been well characterized in the literature,[22] was used as a reference (r). The two-photon absorption cross section of a sample compound (s) can be calculated at each wavelength according to

$$\delta_s = \frac{S_s\eta_r\varphi_r C_r}{S_r\eta_s\varphi_s C_s}\,\delta_r \quad (2)$$

where S is the integrated two-photon induced fluorescence signal, η is the fluorescence quantum yield, C is the concentration of the chromophore, and φ is the overall fluorescence collection efficiency of the experimental apparatus. By measuring the reference and then the sample with minimal delay, φ_r and φ_s can be taken as equal. The concentrations of the solutions were in the range of 5×10^{-6}−6×10^{-6} M. The measurements were conducted in an intensity regime where the fluorescence signal showed a quadratic dependence on the intensity of the excitation beam. The uncertainty in the measured cross sections is about 15%.

2.3.4. Calculation of the Binding Constants. The binding constants K were determined by the fluorescence spectra change using the Benesi−Hildebrand equation.[23]

The equation for the 1:2 complex formation is given by

$$F_0/(F_0 - F) = F_0/(F_0 - F_{complex}) + F_0/(F_0 - F_{complex}) \times 1/K \times 1/[M]^2 \quad (3)$$

where K is the binding constant, F_0 is the integrated fluorescence intensity of free ligand, F is the observed integrated fluorescence intensity, $F_{complex}$ is the emission of the ligand–metal complex, and [M] is the concentration of added metal. When $F_0/(F_0 - F)$ is plotted against the $1/[M]^2$, the binding constant is given by the ratio intercept/slope.

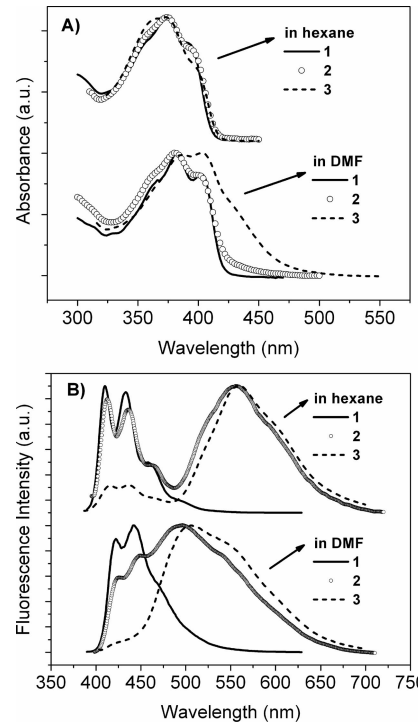

Figure 3. Normalized UV–vis absorbance (A) and emission spectra (B) of **1**, **2**, and **3** in hexane and DMF.

Similarly, the equation for the 1:1 complex formation is given by

$$F_0/(F_0 - F) = F_0/(F_0 - F_{complex}) + F_0/(F_0 - F_{complex}) \times 1/K \times 1/[M] \quad (4)$$

When $F_0/(F_0 - F)$ is plotted against the 1/[M], the binding constant is given by the ratio intercept/slope.

2.3.5. Titration Procedure. To 3.0 mL of 5.6×10^{-6} M solution of the corresponding ligand in DMF was added 3 μL aliquots of metal ions stock solutions (concentration 5×10^{-4}, 5×10^{-3}, 5×10^{-2}, and 0.5 M) or NaOH stock solution (concentration 0.01, 0.1, and 1 M). Upon each addition, the solution was stirred for 5 min to reach equilibrium, and the UV–vis as well as fluorescence spectra were subsequently monitored. A blank experiment was carried out using the same procedure, without metal ions or base to check the effects of added water on photophysical properties. No obvious influence on both the UV–vis and emission spectra was found due to the limited water volume (total added water volume is less than 50 μL).

3. Results and Discussion

3.1. Linear Photophysical Properties. Figure 3 shows the absorption and emission spectra of **1**, **2**, and **3** in hexane and DMF, respectively. In nonpolar hexane, the absorption spectra of **1**, **2**, and **3** (Figure 3A) were analogous to show their similar ground-state properties. However, different absorption spectra were observed in polar DMF. Significant bathochromic shifted absorption spectrum of **3** was observed in DMF as compared to that in hexane, showing its positive solvatochromism. Moreover, dramatically different emission

(21) Joshi, H. S.; Jamshidi, R.; Tor, Y. *Angew. Chem., Int. Ed.* **1999**, *38*, 2721.
(22) (a) Xu, C.; Webb, W. W. *J. Opt. Soc. Am. B* **1996**, *13*, 481. (b) Albota, M. A.; Xu, C.; Webb, W. W. *Appl. Opt.* **1998**, *37*, 7352.
(23) (a) Benesi, H. A.; Hildebrand, J. H. *J. Am. Chem. Soc.* **1949**, *71*, 2703. (b) Fery-Forgues, S.; Le Bris, M.-T.; Guetté, J.-P.; Valeur, B. *J. Phys. Chem.* **1988**, *92*, 6233. (c) Varghese, R.; George, S. J.; Ajayaghosh, A. *Chem. Commun.* **2005**, 593.

Table 1. Some Photophysical Data of 1, 2, and 3, Their Zinc Complexes, and the Deprotonated 3

		one-photon absorption	one-photon fluorescence		two-photon absorption		
symbol	condition	λ_{max} (nm)	λ_{max} (nm)	η^d	λ_{max} (nm)	$\eta\delta$ (GM)	δ (GM)
1	DMF	382	442	0.91	740	110	120
2	DMF	381	494	0.12	740	52	430
2-Zn[a]	DMF + $Zn(OAc)_2$	394	500	0.32	740	85	270
3	DMF	384, 404	499, 559[c]	0.09	740	48	530
3-Zn[a]	DMF + $Zn(OAc)_2$	403, 430[c]	500	0.46	740	215	470
3-O^{-} [b]	DMF + NaOH	441	540	0.32	780	1320	4120

[a] The concentrations of **2** and **3** are 5.6×10^{-6} mol L^{-1} in DMF. The concentration of added zinc ion is 5.6×10^{-5} mol L^{-1}. [b] The concentrations of **3** is 5.6×10^{-6} mol L^{-1} in DMF. The concentration of added NaOH is 9.1×10^{-4} mol L^{-1}. [c] Shoulder. [d] Quantum yield.

spectra (Figure 3B) were observed among the three compounds in nonpolar hexane and polar DMF, showing their different excited states. In hexane, compound **1** exhibits emission bands at 411, 435, and 462 nm, while compound **2** with one HPBO group shows not only slightly bathochromic shifted emissions at 412, 436, and 463 nm but also a broad and featureless emission at 556 nm. Compound **3** with two HPBO groups also shows emission peaks at 413, 436, 463 (very weak), and 559 nm (strong). In comparison with the emission properties of **1** and **2**, the weak high-energy emission bands of **3** at 413, 436, and 463 nm (the normal emission) may be attributed to the excited-state of the rotamers (X4 in Figure 1),[10c,d,11a,c,f] which do not undergo ESIPT. The lower energy band centered at 559 nm, called abnormal emission, results from the ESIPT emission of the keto tautomer (X2). Because of the ESIPT characteristic, a large Stokes shift (187 nm in hexane) is observed for **3** . In DMF, besides the shoulder emission band at ~559 nm (shown in compounds **2** and **3**, Figure 3B) caused by the ESIPT, a strong emission band centered at 499 nm is also observed. On the basis of earlier reports from HPBO-related compoundsin polar solvents,[10d,11g−k] such as DMSO and DMF, the emission band at the intermediate wavelength (499 nm) might be due to the excited-state phenolate anion (X6).[10d,11g−k] A more detailed discussion of the excited-state anion is given in the Supporting Information. Comparing the emission spectra between **2** and **3**, a larger fraction of the normal emission bands is observed in **2**, but a much smaller X6 fraction of **2** in DMF than in **3** because of only a single HPBO unit in **2**. Similarly, the UV–vis absorption spectrum of **2** in DMF shown in Figure 3A was much narrower, and even hypsochromic shifted, compared to that of **3** in DMF, suggesting the structural influence on their linear photophysical properties.

In polar DMF solvent, compound **1** shows strong blue fluorescence with a high quantum yield of 0.91. However, compounds **2** and **3** show weak yellowish fluorescence in DMF with respective quantum yields of 0.12 and 0.09 (Table 1). The low quantum yields of **2** and **3** are possibly due to the nonradiative loss of energy such as the barrierless excited-state intramolecular proton transfer (ESIPT) process of the HPBO moieties or solute–solvent interactions.[10c,24]

3.2. Sensing Properties. *3.2.1. Response with Metal Ions.* Sensing studies were performed in DMF. Compound **1** has no response to the metal ions (not shown here) due to the lack of HPBO moieties. Titration with aqueous $Zn(OOCCH_3)_2$ of solutions of **2** and **3** in DMF induced red shifts in their absorption spectra and a gradual increase of their fluorescence intensities (Figure 4).[25]This indicates the formation of zinc complexes. A single set of isosbestic points were observed from their absorption spectra during the titration, suggesting a simple equilibrium reached in complexation. During the complexation process, the nonradiative loss of energy (as described above) was disrupted, resulting in an enhancement of quantum yield. Quantum yields of 0.46 and 0.32 were obtained at the equilibrium states of **3** and **2** with Zn^{2+} ion, which are 5.2 and 2.7 times greater than those of **3** and **2** before titration. Curve fitting of the fluorescence intensity of **2** against the reciprocal of the Zn^{2+} concentration (1/[M]), the Benesi−Hildebrand plot,[23] gives a linear fit characteristic of a 1:1 complexation behavior from which the association constant is estimated to be 1.0×10^5 M^{-1}. The formation of a 1:1 complex is in accordance with the results of other HPBO materials,[10c,d] whereas the Benesi−Hildebrand plot of the change in emission intensity of **3** against the reciprocal of the square of Zn^{2+} concentration ($1/[M]^2$) gives a linear fit, characteristic of a 1:2 stoichiometry, and yields the binding constant (K) of 3.8×10^9 M^{-2}.[26]

By comparing the fluorescence enhancements against zinc concentration, we found that compound **2** (with one HPBO binding site) is more sensitive than that of **3** (with two binding sites), when the concentration of zinc ion is lower than 1.2×10^{-5} M (point a, shown in Figure 4E). Compound **3** can continue to respond to zinc ion at higher concentrations up to 5.1×10^{-5} M (point b, shown in Figure 4E) because it needs two zinc ions to reach its equilibrium. Since the physical properties of **2** and **3** were altered significantly after the HPBO moiety binds with zinc ion(s), at the equilibrium state, a larger fluorescence enhancement from **3** to **3-Zn** than that from **2** to **2-Zn** was observed. This character also affects their 2PF properties.

The 1PF responses of the three compounds to various metal ions were investigated. The fluorescent response for a certain metal of compounds **2** and **3** is given in Figure 5. At the equilibrium states, **2** and **3** recognize zinc ion(s) to bring about a large fluorescence enhancement, showing their

(24) (a) Grellmann, K. H.; Mordzinski, A.; Heinrich, A. *Chem. Phys.* **1989**, *136*, 201. (b) Yang, G.; Morlet-Savary, F.; Peng, Z.; Wu, S.; Fouassier, J. P. *Chem. Phys. Lett.* **1996**, *256*, 536. (c) Mordzinski, A.; Grellmann, K. H. *J. Phys. Chem.* **1986**, *90*, 5503.

(25) Although the main emission band is the excited state phenolate ion, a blue-shifted emission from the keto tautomer (X2) to the zinc complex (X3) was still observed, which is in generally in accordance with model study.[10b]

(26) Although there were two binding sites in compound **3**, we did not figure out the two-step complexation processes or try to calculate the two binding affinities K_{11} (binding constant with only one Zn^{2+}) and K_{12} (binding constant from the complex with one Zn^{2+} to that with two Zn^{2+}).

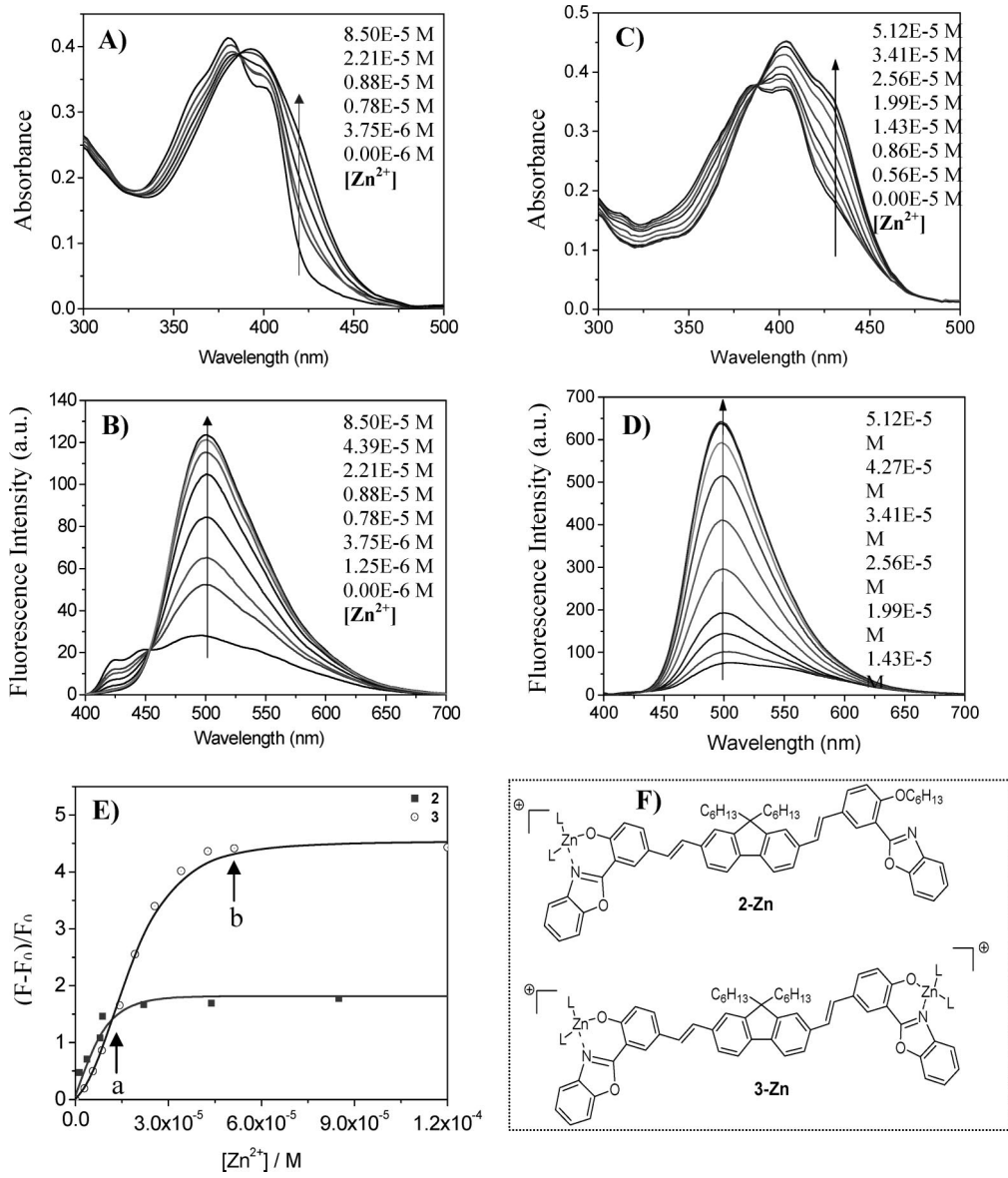

Figure 4. UV–vis spectra (A and C) and fluorescence emission spectra (B and D) of **2** and **3** in 5.6×10^{-6} mol L^{-1} DMF at 25 °C as a function of added $Zn(OOCCH_3)_2$ predissolved in H_2O with various concentrations from 0.0005 to 0.5 M. The emission spectra were excited at the isosbestic point of 387 nm. (A) and (B) are for **2**; (C) and (D) are for **3**. (E) is the sigmoidal plots of the titration processes. (F) gives the zinc complex structures.

unique responses for Zn^{2+} ion, which is necessary and important for an effective chemosensor. Other physiologically important ions, such as Mg^{2+}, Ca^{2+}, Na^{+}, and K^{+}, gave much less enhancement in fluorescence emissions. Lithium ion induced a significant fluorescence enhancement compared to sodium and potassium ions, which may possibly be due to the fact that Li^{+} can also bind with HPBO moiety.[27] The titration of Zn^{2+} in the presence of other metals ions (Mg^{2+}, Ca^{2+}, K^{+}, Na^{+}, and Li^{+}) shows its high selectivity against the other non-Zn^{2+} metal ions (see Supporting Information). However, several heavy metal ions, such as Cu^{2+}, Ni^{2+}, and Fe^{3+}, quench the fluorescence similar to those reported in the literature.[10a,d]

3.2.2. Response with Base. The base (NaOH aqueous solution) stimulated UV–vis and fluorescence properties of compound **3** are shown in Figure 6. Significant red shifts of both its absorption and emission were observed. Furthermore, there is a notable enhancement of its 1PF intensities under basic conditions. These results indicate the deprotonation of the two hydroxyl groups and the formation of the free phenolates (**3**-O^{-} with two X5, Figure 6C) at the equilibrium state. It should be noted that the emission maximum of **3-O**$^{-}$ with free phenolates (X5, ~540 nm) is much more bathochromic shifted than that of **3** with the excited-state phenolate (X6, 499 nm) moieties due to their different ground states. A quantum yield of 0.32 was obtained at the equilibrium state under the basic conditions, which is 3.6 times higher than that of compound **3** (0.09) before titration.

3.3. 2PA Properties. *3.3.1. Response with Zinc Ions.* The two-photon action cross sections ($\eta\delta$, η: quantum yield, δ: two-photon absorption cross section expressed in GM = 1×10^{-50} cm^4 s $photon^{-1}$ $molecule^{-1}$) of compounds **1**, **2**,

(27) (a) Obare, S. O.; Murphy, C. J. *New J. Chem.* **2001**, *25*, 1600. (b) Qin, W.; Obare, S. O.; Murphy, C. J.; Angel, S. M. *Analyst* **2001**, *126*, 1499.

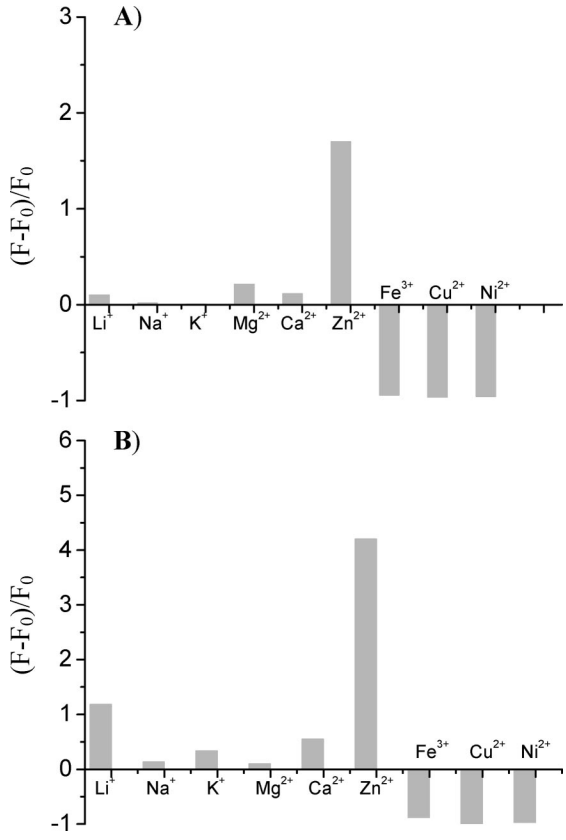

Figure 5. 1PF selectivity of **2** (A) and **3** (B) via various metal ions. Concentrations of **2** and **3** in DMF are 5.6×10^{-6} mol L^{-1}. Concentration of added zinc ion is 5.6×10^{-5} mol L^{-1}. Concentrations of added other metal ions are 5.6×10^{-4} mol L^{-1}. All of the measurements were carried out at the equilibrium states.

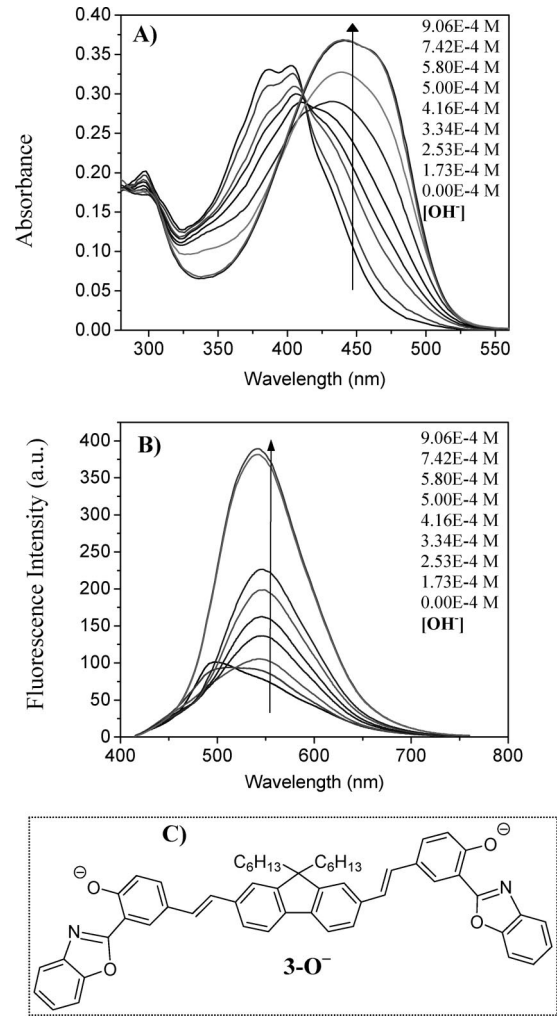

Figure 6. UV–vis spectra (A) and 1PF spectra (B) of **3** during the titration of NaOH aqua. Excitation wavelength for (B) is 414 nm. The structure of the deprotonated **3** (**3-O**$^-$) is given in (C).

and **3** with and without zinc ions were investigated by using a ratiometric two-photon-induced fluorescence measurement technique.[22] Typical results of **3** and its zinc ion equilibrated solution are given in Figure 7. Significant enhancement of the $\eta\delta$ value was observed after the full complexation with Zn^{2+} ion, which may be attributed to the much higher quantum yields of the complexes with zinc ion than those of the free ligands. The titration of **3** and **2** with Zn^{2+} also demonstrated the respective 1:2 and 1:1 complexation, when examined using the 2PF process at 800 nm. The calculated binding constants of **3** and **2** are 3.4×10^9 M^{-2} and 0.94×10^5 M^{-1}, respectively, in accordance with those from 1PF processes. The above results unequivocally prove the possibility of quantitative measurement of the concentration of Zn^{2+} ion from the enhancement of 2PF upon addition of zinc ion to the chromophore-containing solution. On the other hand, similar to the trends of 1PF studies, a unique response for zinc ion in the 2PF process is clearly observed. Compounds **2** and **3** are useful zinc ion sensors using the 2PF process.

3.3.2. Response with Base. When the $\eta\delta$ values of **3** with and without the presence of the NaOH are compared (Figure 8), dramatic enhancement can be observed under basic conditions, indicated by a significant magnification of the maximum 2PA cross sections (δ values) from 530 GM of **3** at 740 nm to 4120 GM of **3-O**$^-$ at 780 nm (Table 1). This is the largest 2PA cross section value reported for the bisphenolate-containing 2PA materials. The value is even bigger than those of some typical 2PA materials (with high δ values of larger than 1000 GM) having substituted dialkylamino groups as the donors.[28] This finding may provide additional information for further optimization of molecular structures of efficient 2PA materials and pH sensors.

3.4. Effect of Molecular Structures on 2PA Cross Sections. The 2PA process is a third-order nonlinear optical property with a strong dependence on the intramolecular charge transfer (ICT) process.[28a,29] The two-photon cross sections of linear or quasi-linear conjugated molecules with a D−π−D motif strongly depend on the donating strength

(28) (a) Albota, M.; Beljonne, D.; Brédas, J. L.; Ehrlich, J. E.; Fu, J. Y.; Heikal, A. A.; Hess, S. E.; Kogej, T.; Levin, M. D.; Marder, S. R.; McCord-Maughon, D.; Perry, J. W.; Röckel, H.; Rumi, M.; Subramaniam, G.; Webb, W. W.; Wu, X. L.; Xu, C. *Science* **1998**, *281*, 1653. (b) Pond, S. J. K.; Rumi, M.; Levin, M. D.; Parker, T. C.; Beljonne, D.; Day, J. M. W.; Brédas, L.; Marder, S. R.; Perry, J. W. *J. Phys. Chem. A* **2002**, *106*, 11470. (c) Mongin, O.; Porres, L.; Moreaux, L.; Mertz, J.; Blanchard-Desce, M. *Org. Lett.* **2002**, *4*, 719. (d) Woo, H. Y.; Korystov, D.; Mikhailovsky, A.; Nguyen, T.-Q.; Bazan, G. C. *J. Am. Chem. Soc.* **2005**, *127*, 13794. (e) Ventelon, L.; Charier, S.; Moreaux, L.; Mertz, J.; Blanchard-Desce, M. *Angew. Chem., Int. Ed.* **2001**, *40*, 2098.

(29) Rumi, M.; Ehrlich, J. E.; Heikal, A. A.; Perry, J. W.; Barlow, S.; Hu, Z.; McCord-Maughton, D.; Parker, T. C.; Röckel, H.; Thayumanavan, S.; Marder, S. R.; Beljonne, D.; Brédas, J. L. *J. Am. Chem. Soc.* **2000**, *122*, 9500.

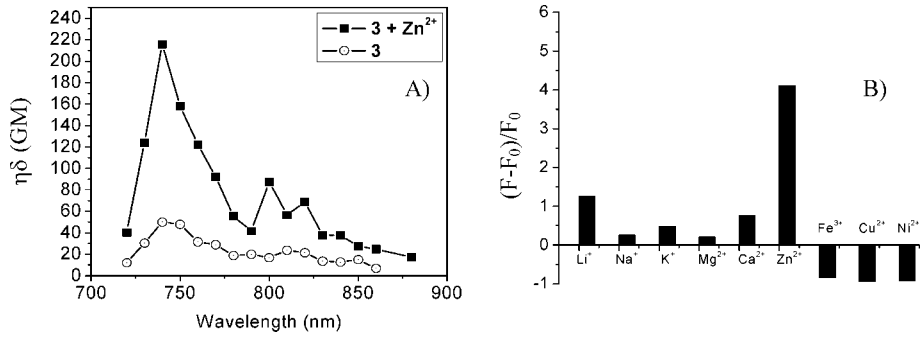

Figure 7. Two-photon action spectra of compound **3** with and without Zn^{2+} ions (A) and the selectivity via various metal ions (B). Concentrations of **3** are 5.6×10^{-6} mol L^{-1} in DMF. The concentration of added zinc ion is 5.6×10^{-5} mol L^{-1}. Concentrations of added other metal ions are 5.6×10^{-4} mol L^{-1}. The selectivity related to two-photon-induced fluorescence process was carried out at 800 nm. F_0 is the integrated fluorescence of free ligand, and F is the integrated fluorescence intensity after the complexation.

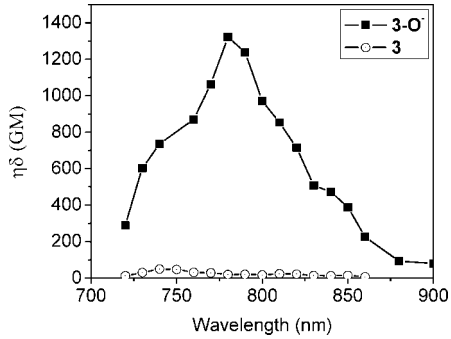

Figure 8. Two-photon action cross-section spectra of **3** with the addition of NaOH aqua (the concentration of added NaOH is 9.1×10^{-4} mol L^{-1} corresponding to 162 equiv of **3**).

and conjugation length. For a given conjugation length, a stronger donor will increase the charge transfer from the ends of molecules to the middle through the reduction of the detuning energy and enhancement of the transition dipole moments, which contributes to a larger δ value due to its stronger ICT process.[28a,29]

The three compounds **1**, **2**, and **3**, their zinc complexes **2-Zn** and **3-Zn** (Figure 4F), and **3-O$^-$** (Figure 6C) have the same conjugation length but different donor end groups (OH, OZn, and OCH_2R; where R = OCH_2OCH_3 for **3** and C_5H_{11} for **1**). Therefore, the materials reported here are a series of compounds used to systematically understand the influence of electron-donating ability on δ values. Note that each compound investigated here has two benzoxazole units, which can act as an electron acceptor to affect the transition dipole moments and modulate the energy differences between transitions. However, since the benzoxazole unit is at the meta-substituted position along the long axis of the D$-\pi-$D or D$-\pi-$D′[30] conjugate, it is not directly conjugated with the rest of chromophore; the contribution of this benzoxazole moiety to the δ values stimulated by zinc ion and base is quite limited.

As for **3-O$^-$**, both the absorbance and emission maxima are significantly red-shifted compared to **3-Zn**, **3**, and **1** (see Table 1), indicating the phenolated (O$^-$) form is a much stronger donor than O$-$Zn, OH, and OCH_2R.[31] Therefore, the strongest donating ability of the free phenolate unit contributes significantly to its large 2PA cross section.

As given in Table 1, the maximum absorbance of **3-Zn**, **2-Zn**, and **1** follows the trend of $\lambda_{3\text{-}Zn} > \lambda_{2\text{-}Zn} > \lambda_1$, indicating the donating ability of the O$-$Zn is larger than OCH_2R. As a result, the δ values of the **3-Zn**, **2-Zn**, and **1** also follow the similar trend of $\delta_{3\text{-}Zn} > \delta_{2\text{-}Zn} > \delta_1$.

It was found that the δ values of **1**, **2**, and **3** follow the trend of $\delta_3 > \delta_2 > \delta_1$. The phenol group is a slightly stronger donating group than the OCH_2R,[31] and **3** also contains a much larger fraction of the excited-state phenonate anion (X6) than that of **2**. All of these factors may contribute significantly to the larger δ value of **3** over **2** and **1**.

Another interesting finding is that the 2PA cross sections of zinc complexes (**3-Zn** and **2-Zn**) are smaller than their corresponding free ligands (**3** and **2**). The free ligand contains a phenol group, which is a weaker donor than the O$-$Zn. According to above discussion, the δ values of the free ligands might be smaller than those of their metal complexes. However, the significant amount of excited-state phenolate ion(s) and ESIPT processes exhibited in **2** and **3** at their excited states may possibly play a significant role in reducing their detuning energy and enhancing their transition dipole moments. As a result, the ligands **2** and **3** exhibit larger δ values than their corresponding zinc complexes.

4. Conclusion

Three novel 2-(2′-hydroxyphenyl)benzoxazole-containing 2PA molecules with 2PA cross sections up to 530 GM were successfully synthesized and characterized. The influence of molecular structures on sensing ability and selectivity for metal ions were investigated by using one- and two-photon-induced fluorescence processes. The sensor **2** with one binding site is more sensitive to a low concentration of zinc ions than the sensor **3** with two binding sites. However, because the binding with zinc ion significantly alter the optical properties, sensor **3**, at its equilibrium state, exhibits

(30) **1**, **3**, **3-Zn**, and **3-O$^-$** can be concerned as the symmetrical D$-\pi-$D 2PA conjugates. **2** and **2-Zn** can be concerned as the asymmetrical D$-\pi-$D′ 2PA conjugates. The 2PA behavior of the asymmetrical D$-\pi-$D′ 2PA conjugate may be more complicated than the D$-\pi-$D motif because the D$-\pi-$D′ structure has more chance to absorb the two individual photons with different energy.

(31) The sigma plus values (σ^+) are -2.3, -0.91, and -0.79 for para-substituted O$^-$, OH, and OCH_3, respectively, indicating the donating ability follows an order of O$^-$ > OH > OCH_3. See: Hine, J. In *Structural Effects on Equilibria in Organic Chemistry*; John Wiley: New York, 1975; p 72.

a larger fluorescence enhancement than **2**. The two compounds **2** and **3** show a good selectivity for zinc ion in both 1PF and 2PF processes. It was also found that both the 1PF and 2PF properties of compound **3** were affected dramatically by base, indicating the compound may also possibly act as a pH sensor. Interestingly, when stimulated by base, the deprotonated compound **3** (**3-O**$^-$) exhibits a very large two-photon absorption cross section of 4120 GM at 780 nm in DMF. This is the largest δ value reported so far for a bisphenolate-containing 2PA material. Through an analysis of the photophysical properties and molecular structures, it was found that the donating groups in these molecules, including the ligands, zinc complexes, and phenolate anion(s), play a significant role in determining the 2PA cross sections. The trend of two-photon cross sections of the chromophores demonstrated the electron-donating ability of substitution group in the sequence of $-O^-$ > $-OZn$ > $-OCH_2R$. The limitation of the compounds studied in this paper for bioapplication is their hydrophobic properties. In order to make them really applicable in biological environments, the materials should be water-soluble and cell-permeable for the intracellular sensing. We are modifying the compounds with poly(ethylene glycol) and sugar to improve their biocompatibility and cell permeability. Results will be reported in the coming publications.

Acknowledgment. Financial support from the National Science Foundation (the NSF-STC program under Agreement DMR-012-0967) and the Microscale Life Science Center, an NIH Center of Excellence at the University of Washington (5 P50HG002360-04), is acknowledged.

Supporting Information Available: UV–vis and fluorescence spectra of **3** in hexane, DMF, and acidic DMF, two-photon action cross sections of **1** and **2**, 2PF selectivity via various metal ions, 1PF selectivity of Zn^{2+} against other metal ions, Benesi−Hildebrand plots, and NMR spectra of all of the new compounds. This material is available free of charge via the Internet at http://pubs.acs.org.

CM702527M